


Concept Paper

# Structural Analysis of the BaWO<sub>4</sub> Crystal Doped with Ce and Codoped with Na Ions Based on g-shift Parameters

Tomasz Bodziony \*  and Sławomir Maksymilian Kaczmarek 

Institute of Physics, Faculty of Mechanical Engineering and Mechatronics, West Pomeranian University of Technology, Al. Piastów 17, 70-310 Szczecin, Poland; skaczmarek@zut.edu.pl

\* Correspondence: tbodziony@zut.edu.pl

Received: 31 July 2020; Accepted: 4 September 2020; Published: 6 September 2020



**Abstract:** The relationship between the g-shift and the local structure of the Ce<sup>3+</sup> paramagnetic center with axial symmetry were investigated for four BaWO<sub>4</sub> single crystals doped with Ce and codoped with Na. Based on g-shift the displacements of Ce<sup>3+</sup> ions are determined. The g-shift method yields displacements of impurity ions in good agreement with the superposition model (SPM) and the perturbation methods (PM) predictions. The structural analysis of the paramagnetic ions and its surrounding in the BaWO<sub>4</sub> unit cell was also conducted.

**Keywords:** g-shift; axial symmetry; EPR; BaWO<sub>4</sub>

## 1. Introduction

In recent years, ABO<sub>4</sub> compounds have attracted a great deal of interest due to their applications. The wolframite and scheelite structures are common structure types for ABO<sub>4</sub> compounds [1]. Tungstate materials like BaWO<sub>4</sub>, PbWO<sub>4</sub>, CaWO<sub>4</sub>, or SrWO<sub>4</sub> are very interesting because of their applications as laser host material or scintillators. Among the tungstate materials barium tungstate (BaWO<sub>4</sub>, BWO) is a very attractive inorganic optical material due to its emission properties and its potential as a material for stimulated Raman scattering for application in Raman shifters [2] of laser radiation or as scintillators and X-ray phosphor [3].

Doped barium tungstate single crystals with alkali earth metals (Me) or rare-earth ions (Re) display the greater possibility of further applications as luminescence and solid-state laser materials. Doping with trivalent ions to make them applicable and requires charge compensation which may be provided, for example, by structural defects or proper codoping with alkaline metal ions. Voronina et al. have obtained BaWO<sub>4</sub>: Nd<sup>3+</sup> single crystals by the Czochralski method using compensating dopants: Nb<sup>5+</sup>, Na<sup>+</sup> [4]. Liao et al. [5] performed chemical analyses of the BaWO<sub>4</sub>: Pr<sup>3+</sup> microcrystalline samples by energy-dispersive X-ray spectroscopy (EDS). Na<sup>+</sup>, Pr<sup>3+</sup>, Ba<sup>2+</sup>, W and O were detected for all samples. Moreover, the Pr<sup>3+</sup> content was nearly equal to the Na<sup>+</sup> content. They supposed that the charge compensation mechanism of BaWO<sub>4</sub>: Pr<sup>3+</sup> phosphors may be such that two Ba<sup>2+</sup> ions are replaced by one Pr<sup>3+</sup> ion and one Na<sup>+</sup> ion, 2Ba<sup>2+</sup> = Pr<sup>3+</sup> + Na<sup>+</sup>. The charge compensation pattern has been discussed in detail in the case of Eu<sup>3+</sup> and Na<sup>+</sup> codoped CaWO<sub>4</sub> phosphors [6]. The hypothesis of Codoping of Eu<sup>3+</sup> and Na<sup>+</sup> at Ca<sup>2+</sup> sites were verified, too [6]. Kaczmarek et al. published another paper about Pr<sup>3+</sup> and Na<sup>+</sup> sites in BaWO<sub>4</sub> single crystals doped with Pr and codoped with Na [7].

The doping process with different RE ions leads to different optical or magnetic properties of the doped hosts. The application of different methods may lead to different structural defects in grown crystals and changed optical properties. We decided to codope BaWO<sub>4</sub>: Ce single crystals with Na ions using the Czochralski growth method with inductive heating [8,9]. A deeper understanding

of the influence of structural properties of BWO on their luminescent behavior and electro-optical properties is crucial for their applications [10,11]. The understanding is particularly important in the case of doped BaWO<sub>4</sub> single crystal. Doped barium tungstate single crystals with alkali earth metals (Me) or rare-earth ions (Re) greatly increases the further possibility of application as luminescence and solid-state laser materials. Currently, many papers are focused on the investigation of BWO thin films or the synthetization of nanoscale rods, cylinders made of BaWO<sub>4</sub> [12,13]. However, there are a few papers that deal with doping, absorption bands or defect study of barium tungstate (BaWO<sub>4</sub>) crystal [14–16].

BWO crystal with scheelite structure crystallized in the tetragonal space group with C<sub>6h</sub><sup>2</sup> (I4<sub>1</sub>/a) [17]. Lattice parameters of BWO are:  $a = b = 5.6148 \text{ \AA}$ ,  $c = 12.721 \text{ \AA}$  [1,17] (see Figure 1). Both Ba<sup>2+</sup> and W<sup>6+</sup> sites have S<sub>4</sub> point symmetry. In the tungstate compound, Ba<sup>2+</sup> is coordinated by eight O<sup>2-</sup> ions in the form of a dodecahedron [BaO<sub>8</sub>] made of two rotated, interpenetrated tetrahedra (see Figure 2). The distance Ba–O is 2.7857 Å and 2.8310 Å, respectively, for two tetrahedra forming a dodecahedron [BaO<sub>8</sub>]. The [WO<sub>4</sub>] tetrahedron has a nearby regular shape only slightly distorted along the c (S<sub>4</sub>) axis. In the tetrahedron [WO<sub>4</sub>], the W–O bond length is 1.8230 Å [1]. All data for pure, undoped lattice structure. In the c (z) directions, [BaO<sub>8</sub>] dodecahedra are connected by its edges. Barium dodecahedra [BaO<sub>8</sub>] and tungsten tetrahedra [WO<sub>4</sub>] are connected by O atoms. Therefore, each O atoms links with two Ba atoms and one W atom. It is worth mentioning that the volume of the cell BaWO<sub>4</sub> is the greatest one among ABO<sub>4</sub> molybdates and tungstate with the structure of wolframite and scheelite, according to Sleight ( $V = 401.0 \text{ \AA}^3$ ) [1].

For a cerium ion (Ce<sup>3+</sup>, f<sup>1</sup> electronic configuration) in tetragonal symmetry, its <sup>2</sup>F<sub>5/2</sub> ground state would be split into tree Kramers doublets. Only the lowest doublet is populated. Therefore, the Ce<sup>3+</sup> ion has an effective spin  $S = 1/2$ . This article continues our previous papers related to the investigation of BaWO<sub>4</sub> single crystals doped with Ce and codoped with Na [8,9]. Barium tungstate doped and codoped with cerium and sodium (BaWO<sub>4</sub>: Ce, Na) with different amounts of impurities were investigated by Electron Paramagnetic Resonance (EPR). New paramagnetic centers with axial or lower symmetry were detected and spin Hamiltonian parameters were established [8,9]. A few articles about investigations of BWO doped and codoped with different elements were found. Kunti et al. published an article about BaWO<sub>4</sub> doped with Dy<sup>3+</sup> and codoped with K<sup>+</sup> (Ba<sub>1-x-y</sub>Dy<sub>x</sub>K<sub>y</sub>WO<sub>4</sub> ( $x = 0.10$ ;  $y = 0.05$ )) [14]. However, they focused on optical and XRD measurements with detailed structural analysis, without EPR data and analysis [14].

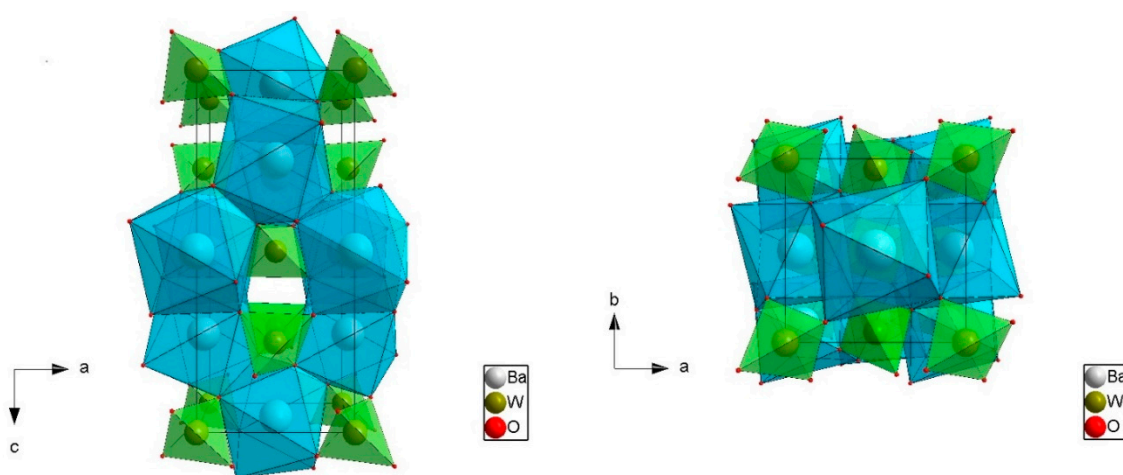


**Figure 1.** Unit cell structure of BaWO<sub>4</sub> viewed along the b-axes (left) and c-axes (right) with marked dodecahedra [BaO<sub>8</sub>] (blue) and tetrahedra [WO<sub>4</sub>] (green).

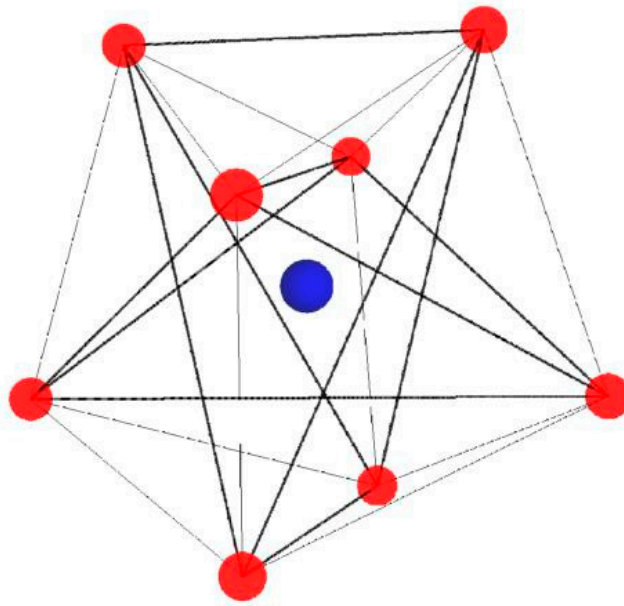


**Figure 2.** Fragment of the barium tungstate (BWO) cell structure: dodecahedron [BaO<sub>8</sub>] consisting of two rotated tetrahedra.

The EPR measurements is a sensitive method to detect a local surrounding of the impurity ions. An impurity ion serves as a probe to study local surroundings. However, the extraction of more detailed structural information from EPR spectra such that one about lattice distortion around an impurity ion is not an easy task. Generally, there are two methods of obtaining this kind of information from spin—Hamiltonian parameters calculated on the basis of ERP measurements: (a) superposition model (SPM) [18] and/or (b) perturbation methods (PM) up to second-order (or higher) [19]. However, only  $g$ -parameters were calculated for BaWO<sub>4</sub>: Ce, Na single crystals. There are  $g_{\parallel}$ ,  $g_{\perp}$  for axial symmetry centers, and  $g_x$ ,  $g_y$ ,  $g_z$  for lower symmetry centers [8,9]. Therefore, the use of the SPM model is impossible. Nevertheless, a simplified method proposed by Newman can be used [20]. Newman suggested a method to extract structural information from the  $g$ -shift parameters [18,20]. In this paper, his method will be applied to results already published in previous articles [8,9,21]. The goal is to find out where the dopant ions are located in the host crystal and the changes in their surroundings. Those results will be analysed on the basis of crystallographic data and other publications.

## 2. Theoretical Background

The spin Hamiltonian (SH) may be written as [22,23]:

$$\hat{H} = \mu_B (\vec{B} \cdot \hat{g} \cdot \hat{J}) + \sum_{k,q} B_k^q O_k^q \quad (1)$$

where  $O_k^q$  is a spin operator,  $B_k^q$  is crystal field parameters, where  $k = 2, 4, 6$ ,  $|q| \leq k$ ,  $J$  is an angular momentum, assuming the absence of the hyperfine structure. Equation (1) is applied both to transition metal ions (TM) and rare-earth ions (RE) except for the replacement of  $J$  by  $S$  for transition metal (TM) ions [22]. The Zeeman term in case the axial symmetry is given by [22]:

$$\hat{H}_Z = \mu_B [g_{\parallel} B_z J_z + g_{\perp} (B_x J_x + B_y J_y)] \quad (2)$$

In SPM model,  $g_{ij}$  factors are the sum of contributions from surrounding ligands [18,20]:

$$\Delta g_{\alpha\beta} = \sum_{\text{ligands } i} K_{\alpha\beta}(i) \Delta \bar{g}(i) \quad (3)$$

where  $\Delta g$  is a g-shift.  $K_{\alpha\beta}(i)$  parameters are determined by the angular coordination of ligands  $i$ .  $\Delta\bar{g}(i)$  are parameters depend only on distance from ligand. The transformation properties of  $\Delta g_{\alpha\beta}$  gives the expressions for  $K_{\alpha\beta}(i)$  in terms of angular position of ligands in spherical polar coordinates  $(\theta, \Phi)$ . Coordination factors  $K_{\alpha\beta}$  are given in Appendix A. Coordination factors  $K_2^0$  can be obtained from the relation [20]:

$$K_2^0 = \frac{1}{2}(K_{xx} + K_{yy} - 2K_{zz}) = \frac{1}{4}(1 + 3\cos 2\theta) \quad (4)$$

The parameter  $K_2^0[\theta]$  is just a function of polar angle  $\theta$ . In the SPM model, g-shift depends on the ratio  $(\Delta g/D)$  [19]. However, Newman proposed the following formulae defining the normalizing g-shift as a function of  $\theta$  angle [20]:

$$\frac{g_{\perp} - g_{\parallel}}{g - g_0} = \frac{3}{2}K_2^0[\theta] \cdot n \quad (5)$$

where  $g_0 = 2.0023$  is the free-ion value,  $g = \frac{1}{3}(2g_{\perp} + g_{\parallel})$  mean value and  $n$  is a number of ligands [20]. In Equations (4) and (5), only the polar angle ( $\theta$ ) is present. One polar angle suffices for a partial description of an ion–host system and its deformations. Figure 3 shows the  $\text{WO}_4$  tetrahedron taken from the BWO unit cell. The two marked angles O–W–O (upper and lower) are equal and their value is  $2\theta_1 = 2\theta_2 = 112.4^\circ$ . The axis symmetry (c-axis) is marked too.

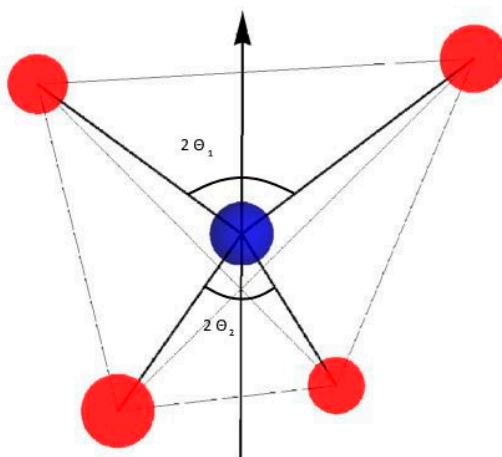


Figure 3.  $[\text{WO}_4]$  tetrahedron with marked angles O–W–O and c-axes.

If  $\theta_1 = \theta_2$ , the tungstate (W) ion is placed in the middle of the tetrahedron  $[\text{WO}_4]$  and the system has cubic symmetry. Other data suggest that the tetrahedron  $[\text{WO}_4]$  is slightly distorted, and  $\theta_1 \cong \theta_2$ . If the tungsten ion is shifted along the axis symmetry these angles will become different ( $\theta_1 \neq \theta_2$ ) the system will display an axial symmetry. If tungsten ion moves out of the c-axis, the  $\text{WO}_4$  system will have lower symmetry than axial. Finally, one parameter (e.g., the angle  $\theta$  to the positive axis symmetry) describes the position of the impurity ion on the axis symmetry in the oxygen tetrahedron or dodecahedron with axial symmetry. The value of this angle describes the position and the displacement of the ion from the midway plane. Detailed crystallographic analysis is also necessary because any mathematical model can give results without physical sense. Of course, the polar angle  $\theta$  includes only a part of the structural information about axial symmetry systems. We cannot conclude from it anything about azimuthally angles ( $\varphi$ ) or the rotation angle of the lower oxygens.

### 3. Results and Discussion

The following  $\text{BaWO}_4$  single crystals were investigated by EPR in previous papers: (a)  $\text{BaWO}_4$ : 0.5% at. Ce, (b)  $\text{BaWO}_4$ : 1.0% at. Ce, (c)  $\text{BaWO}_4$ : 0.5% at. Ce, 1.0% at. Na and (d)  $\text{BaWO}_4$ : 1.0% at. Ce, 2.0% at. Na [8,9]. Two crystals were doped with cerium, two were doped with cerium and codoped with sodium. One axial symmetry ( $S_4$  or  $D_{2d}$ ) paramagnetic center was found present in all four single

crystals, and ten lower symmetry centers ( $C_2$ ) were identified [8,9]. Some centers clearly differ in the values of g parameters ( $g_x \neq g_y \neq g_z$ ). However, some other centers have similar values ( $g_x \cong g_y \neq g_z$ ) Table 1 collects original data for those, selected paramagnetic centers with similar values of ( $g_x \cong g_y$ ) taken from [8,9].

**Table 1.** Hamiltonian parameters of  $Ce^{3+}$  ions, g-factors in the  $BaWO_4$  crystal for selected centers, data from [8,9].

	<b>BaWO<sub>4</sub>:</b>	<b>g<sub>x</sub></b>	<b>g<sub>y</sub></b>	<b>g<sub>z</sub></b>	<b>Symmetry</b>
1	All four samples	1.506(1)	1.506(1)	2.712(2)	$C_4$
2	1.0% at. Ce	1.38(2)	1.35(1)	2.39(1)	$C_2$
3	0.5% at. Ce, 1.0% at. Na	1.44(1)	1.46(1)	2.65(1)	$C_2$
4	0.5% at. Ce, 1.0% at. Na	1.48(1)	1.49(1)	2.68(1)	$C_{2v}$
5	1.0% at. Ce, 2.0% at. Na	1.48(1)	1.44(1)	2.69(1)	$C_{2v}$

The paramagnetic center with axial symmetry (Number 1 is strong and present in all four BWO single crystals. Centers 2–5 with lower symmetry are present only in selected  $BaWO_4$  single crystals. In previous papers only Zeeman term was taken into account in spin—Hamiltonian without crystal field terms which additionally may have increased the error of calculated values of g-parameters [8,9]. The values of  $g_x$  are equal to  $g_y$  (within the error limit) or very close for all five centers (see Table 1). Therefore, one can assume that all centers from Table 1 have axial symmetry ( $g_x = g_y \neq g_z$ ). Table 2 gathers g-parameters for  $Ce^{3+}$  centers with axial symmetry. It was assumed that the g perpendicular  $g_{\perp} = g_z$  and g parallel is on average  $g_{\parallel} = \frac{1}{2}(g_x + g_y)$ .

**Table 2.** The values of g-parameters of  $Ce^{3+}$  centers with axial symmetry in the  $BaWO_4$  crystal. Based on the data from [8,9] assuming that  $g_{\perp} = g_z$ ,  $g_{\parallel} = \frac{1}{2}(g_x + g_y)$ .

	<b>BaWO<sub>4</sub>:</b>	<b>g<sub>  </sub></b>	<b>g<sub>⊥</sub></b>	<b>Symmetry</b>
1	All four samples	1.506(1)	2.712(2)	axial
2	1.0% at. Ce	1.365(20)	2.390(10)	axial
3	0.5% at. Ce, 1.0% at. Na	1.450(20)	2.650(10)	axial
4	0.5% at. Ce, 1.0% at. Na	1.485(20)	2.680(10)	axial
5	1.0% at. Ce, 2.0% at. Na	1.460(20)	2.690(10)	axial

We can now use Equation (5) to determine the position of the impurity ion ( $Ce^{3+}$ ) and its displacement. In the literature, it is generally accepted that trivalent rare-earth dopant ions (e.g.,  $Ce^{3+}$ , or  $Er^{3+}$ ) are located on the barium ion ( $Ba^{2+}$ ) site and preserve the tetragonal site symmetry ( $S_4$ ) [8,9,14,24]. Of course, the charge compensation is necessary. The same is applied to F type color centers, or color centers in BWO [15,16]. Rare-earth ions like cerium ( $Ce^{3+}$ ) or erbium ( $Er^{3+}$ ) cannot located on the  $W^{6+}$  site because of the charge compensation and ionic radii. The ionic radii data are collected in Table 3, according to Shannon [25]. Radii  $Dy^{3+}$  and  $K^+$  ions were added for comparison to the paper by Kunti et al. [14].

**Table 3.** Ionic radii data, according to Shannon [25].

Ba <sup>2+</sup> 6, 8 Coordinate	W <sup>6+</sup> 4, 6 Coordinate	Ce <sup>3+</sup> 6, 8 Coordinate	Na <sup>+</sup> 6, 8 Coordinate	Dy <sup>3+</sup> 6, 8 Coordinate	K <sup>+</sup> 4, 8 Coordinate
1.35, 1.42 Å	0.42, 0.6 Å	1.01, 1.143 Å	1.02, 1.18 Å	0.912, 1.027 Å	1.38, 1.51 Å

The polar angles ( $\theta$ ) were calculated for Ce<sup>3+</sup> centers in BWO single crystals based on the structural parameters. The polar angles ( $\theta_i$ ) were calculated using Equation (5). The results have been composed together in Table 4. The host polar angles  $\theta_i$  were collected in Table 4, too (first row, Table 4). Calculations were made for: (a) dodecahedra [CeO<sub>8</sub>], assuming that Ce<sup>3+</sup> ion substitutes the Ba<sup>2+</sup> site,  $n = 8$  and (b) tetrahedra [CeO<sub>4</sub>] assuming that Ce<sup>3+</sup> ion substitutes W<sup>6+</sup> site,  $n = 4$ , where  $n$  is number of ligands. The polar angles  $\theta_1, \theta_2$  are angles between Ba-O (W-O) and the  $c$ -axes, respectively (see Figure 3).

**Table 4.** The values of polar angles ( $\theta$ ) for Ce<sup>3+</sup> centers in BaWO<sub>4</sub> single crystals for dodecahedra [CeO<sub>8</sub>] and the tetrahedron [CeO<sub>4</sub>] (grey background).

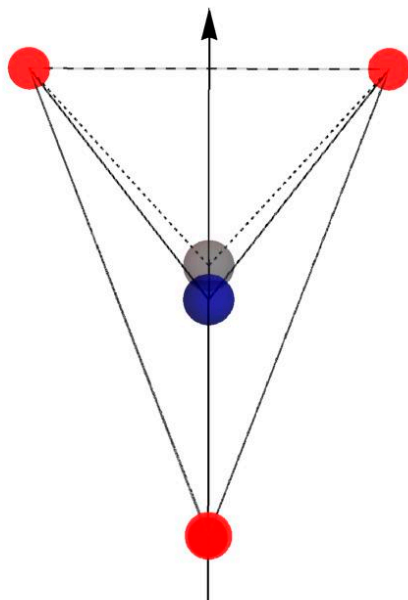
		$\theta_1$ Dodecahedron (in degrees)	$\theta_2$ Tetrahedron (in degrees)	$\Delta\theta = \theta_{calc} - \theta_{1,2}$
	BaWO <sub>4</sub> , pure host	37.7	56.2	-
1	all four samples	42.1(1)	28.7(1)	4.4(1) -27.5(1)
2	BaWO <sub>4</sub> : 1.0% at. Ce	40.1(2)	63.4(2)	2.4(2) 7.2(2)
3	0.5% at. Ce, 1.0% at. Na	39.3(3)	21(3)	1.6(3) -35.2(3)
4	0.5% at. Ce, 1.0% at. Na	40.9(3)	25.9(3)	3.2(3) -30.3(3)
5	BaWO <sub>4</sub> : 1.0% at. Ce, 2.0% at. Na	40.4(2)	24.7(2)	2.7(2) -31.5(2)

Figure 4 shows [BaO<sub>4</sub>] and [CeO<sub>4</sub>] tetrahedra with marked angles O-Ba-O, O-Ce-O and  $c$ -axes. The dodecahedron [BaO<sub>8</sub>] is made of two rotated, interpenetrated tetrahedra (see Figure 2). The Figure 4 presents the displacement of the dopant ion (Ce<sup>3+</sup>, gray color) with respect to the Ba ion (blue color) in one of the [BaO<sub>4</sub>] tetrahedrons for axial center presents in all, four measured samples (number 1, white background, Table 4).

Let us examine the results of the calculations in Table 4, which contains two groups of results, the first of which for when it was assumed that the cerium ion (Ce<sup>3+</sup>) substitutes the Ba<sup>2+</sup> site in the dodecahedron [BaO<sub>8</sub>] for all four BaWO<sub>4</sub> single crystals with different amounts of impurities. The second group is for when the cerium ion (Ce<sup>3+</sup>) substitutes the W<sup>6+</sup> site in the tetrahedron [WO<sub>4</sub>] (Table 3, lines, grey background). The last column shows the difference between the calculated angle and the structure angle, respectively, for the barium dodecahedron and tungsten tetrahedron. The angular distortion for dodecahedra [CeO<sub>8</sub>] is within a few degrees, from 1.6° to 4.4° for BaWO<sub>4</sub>: 0.5% at. Ce, 1.0% and BaWO<sub>4</sub>: 0.5% at. Ce, Na, respectively. One can see that the Ce<sup>3+</sup> ion only slightly shifts along the  $c$ -axes (see Figure 4). The dodecahedron [BaO<sub>8</sub>] is made of two rotated, interpenetrated tetrahedra (Figure 2). We get only one polar angle. However, the results qualitatively describe the distortion of the [CeO<sub>8</sub>] dodecahedron.

Shao-Yi and Hui-Ning published an article about theoretical investigations of the ERP  $g$  factor and the local structure for Er<sup>3+</sup> ions in BaWO<sub>4</sub> [24]. They used the full SPM model for calculation and estimated the angular distortion  $\Delta\theta \cong 1.5^\circ$  for the erbium ion (Er<sup>3+</sup>) in BaWO<sub>4</sub> [24]. They also assumed that Er<sup>3+</sup> ions substitute Ba<sup>2+</sup> in the dodecahedron [BaO<sub>8</sub>]. We used a simplified model based on  $g$ -shift parameters for different rare-earth ions. Nevertheless, we can say that our results are quantitatively

consistent. The angular distortion data obtained from the g-shift parameters' model confirm that  $\text{Ce}^{3+}$  ion substitutes the  $\text{Ba}^{2+}$  site in the dodecahedron  $[\text{BaO}_8]$  for all  $\text{BaWO}_4$  single crystals and shows only a small displacement along c-axes (see Table 4).



**Figure 4.**  $[\text{BaO}_4]$  and  $[\text{CeO}_4]$  tetrahedra with marked angles O-Ba-O, O-Ce-O and c-axes.

The second data group, when the cerium ion ( $\text{Ce}^{3+}$ ) substitutes the  $\text{W}^{6+}$  site in the tetrahedron  $[\text{WO}_4]$  looks quite different (Table 4, lines with a gray background). The angular distortions have a negative sign and quite large values, approximately  $\Delta\theta \approx -30^\circ$ . It means that the tetrahedron  $[\text{CeO}_4]$  would be strongly distorted.  $\text{Ce}^{3+}$  would be shifted approximately to the upper (or lower) limit of the tetrahedron (see Figure 3). Therefore, the tetrahedron  $[\text{CeO}_4]$  should be discarded. However, there is one exception. The angular distortion is  $\Delta\theta \approx 7^\circ$  for  $\text{BaWO}_4$ : 1.0% at. Ce (see Table 4). This result looks quite reasonable. It suggests a slight shift of the  $\text{Ce}^{3+}$  ion along c-axes in the tetrahedron  $[\text{CeO}_4]$  comparable to shifts in the dodecahedron  $[\text{CeO}_8]$ . This result should not be a priori rejected but should be subjected to a deeper analysis. Table 5 presents summary data based on g-shift parameter calculations. Positive sign (+) means that  $\text{Ce}^{3+}$  ion can substitute  $\text{Ba}^{2+}$  or  $\text{W}^{6+}$  ions. The negative sign (−) means that  $\text{Ce}^{3+}$  ion cannot substitute  $\text{Ba}^{2+}$ , or  $\text{W}^{6+}$  sites in the dodecahedron  $[\text{BaO}_8]$  or tetrahedron  $[\text{WO}_4]$ , respectively.

**Table 5.** Summary data:  $\text{Ce}^{3+}$  ion in the dodecahedron  $[\text{BaO}_8]$  or the tetrahedron  $[\text{WO}_4]$  in  $\text{BaWO}_4$  single crystals.

$\text{BaWO}_4$ :	0.5% at. Ce	1.0% at. Ce	0.5% at. Ce, 1.0% at. Na	0.5% at. Ce, 1.0% at. Na	1.0% at. Ce, 2.0% at. Na
Dodecahedron $[\text{BaO}_8]$	+	+	+	+	+
Tetrahedron $[\text{WO}_4]$	−	+	−	−	−

+ possible, − impossible.

Obtained results confirm that impurity ion (i.e.,  $\text{Ce}^{3+}$ ) can substitute the  $\text{Ba}^{2+}$  site, and generally cannot substitute the  $\text{W}^{6+}$  site in BWO crystal [8,9,14–16,24]. However, relatively small angular distortion for  $\text{BaWO}_4$ : 1.0% at. Ce may suggest the existence of such a possibility. Why is the  $\text{Ce}^{3+}$  ion (i.e.,  $\text{Ce}^{3+}$ ) unable to substitute the  $\text{W}^{6+}$  site in the BWO cell? There are two problems with such substitutions: ionic radii and charge compensations. The  $\text{W}^{6+}$  ion has the smallest ionic radii. Barium ion ( $\text{Ba}^{2+}$ ) is approximately three times greater: 0.42 Å (4 coordinate) and 0.6 Å (8 coordinate)

respectively (Table 3). The distance Ba–O is equal  $\cong 2.8$ , which is 156% greater than W–O ( $\cong 1.8$  Å). Therefore, there is much more space for a dopant ion in the dodecahedron [BaO<sub>8</sub>] than in the tetrahedron [WO<sub>4</sub>]. The charge compensation is achieved by vacancies on the barium site ( $V_{Ba}$ ) [14–16,24]. However, there are oxygen ions sharing among the dodecahedron [BaO<sub>8</sub>] and tetrahedron [WO<sub>4</sub>]. Each oxygen O ion links with two Ba and one W ions. In the tetrahedron [WO<sub>4</sub>], each oxygen O ion links to two dodecahedra [BaO<sub>8</sub>] connected by the edge. In the case of vacancies on the barium site ( $V_{Ba}$ ), the bond angle and bond length of the B–O and W–O changes. It causes distortion in the dodecahedron [BaO<sub>8</sub>] and tetrahedral structure of [WO<sub>4</sub>] [14]. In the case of two pairs of barium vacancies ( $V_{Ba}$ ) (each pair [BaO<sub>8</sub>] linked to two upper (or lower) oxygen ions in the tetrahedron [WO<sub>4</sub>] (see Figure 3) the displacement of these two O ions can make enough space to substitute tungsten by impurity ions ( $Ce_W$ ). Additionally, this new paramagnetic center would show an axial symmetry. The biggest volume of unit cell among ABO<sub>4</sub> molybdates and tungstates [1] from which comes the relative flexibility of the unit cell structure BaWO<sub>4</sub> can also be helpful. Ions of second dopant (i.e., Na<sup>+</sup>) substitute also Ba<sup>2+</sup> site ( $Na_{Ba}$ ). Barium vacancies ( $V_{Ba}$ ) and codopant sites ( $Na_{Ba}$ ) guarantee compensation mechanism and new cerium ( $Ce_W$ ) centers are strongly forbidden. Therefore, the new possible paramagnetic center can be present in the case of BaWO<sub>4</sub> with a significant amount of impurities, BaWO<sub>4</sub>: 1.0% at. Ce. The  $Ce_W$  paramagnetic centers can be observed only in EPR measurements, not in optics or XRD measurements. Of course, this is only a theoretical explanation of one computational result therefore more evidence is needed. However, the dopant ion in the tungsten tetrahedron [WO<sub>4</sub>] may be one of the reasons for the increase in the lattice volume of the unit cell reported by Kunti et al. [14]. Each larger dopant ion ( $Ce^{3+}$  or  $Dy^{3+}$ ) will push out oxygens influencing via oxygens on the surrounding dodecahedra. The volume of the unit cell increases as a result. The influence of the dopant and codopant in the case of a significant amount of impurities, such as those reported by Kunti et al. [14], should be subject to further investigations.

#### 4. Conclusions

The values of g-parameters were published previously for two doped with rare-earth cerium ( $Ce^{3+}$ ) ions and two additionally codoped with sodium ions (Na): (a) BaWO<sub>4</sub>: 0.5% at. Ce, (b) BaWO<sub>4</sub>: 1.0% at. Ce, (c) BaWO<sub>4</sub>: 0.5% at. Ce, 1.0% at. Na and (d) BaWO<sub>4</sub>: 1.0% at. Ce, 2.0% at. Na [8,9]. One axial symmetry paramagnetic center was found, and ten with lower symmetry centers were identified previously. Five new, paramagnetic centers ( $Ce^{3+}$ ) with axial symmetry were suggested after a deeper analysis (Table 2). A method to extract structural information from g-shift, proposed by Newman, was used [20]. The following assumptions were made: (a) cerium ion ( $Ce^{3+}$ ) substitutes the Ba<sup>2+</sup> ion in the dodecahedron [BaO<sub>8</sub>], (b) ion ( $Ce^{3+}$ ) substitutes W<sup>6+</sup> ion in the dodecahedron tetrahedron [WO<sub>4</sub>]. On the basis g-shift model for all paramagnetic centers with axial symmetry the polar angles of the oxygen ions making dodecahedron [BaO<sub>8</sub>] and tetrahedron [WO<sub>4</sub>], respectively, were calculated.

Results of calculations display that the angular distortions for dodecahedra [CeO<sub>8</sub>] are within a few degrees, in the range from 1.6° to 4.4° for BaWO<sub>4</sub>: 0.5% at. Ce, 1.0% at. Na and BaWO<sub>4</sub>: 0.5% at. Ce, respectively. There is a quantitative consistency of our results with other results already present in the literature which were obtained by applications of the superposition model (SPM) for erbium ions ( $Er^{3+}$ ) in BaWO<sub>4</sub> [24]. However, we used a simplified g-shift model. The angular distortion data obtained from the g-shift model confirm that  $Ce^{3+}$  ion substitutes the Ba<sup>2+</sup> site in the dodecahedron [BaO<sub>8</sub>]. In the case of cerium ion ( $Ce^{3+}$ ) substitutes the W<sup>6+</sup> site in the tetrahedron [WO<sub>4</sub>] the angular distortions have a negative sign and quite large values, approximately  $\Delta\theta \approx -30^\circ$ . Therefore, the tetrahedron [CeO<sub>4</sub>] should be discarded. However one exception was observed. The angular distortion is equal  $\Delta\theta \approx 7^\circ$  for BaWO<sub>4</sub>: 1.0% at. Ce (see Table 3). It is generally accepted that impurity ions, like rare-earth ions, cannot substitute tungsten (W) in the tetrahedron [WO<sub>4</sub>] in BaWO<sub>4</sub> crystal. Nevertheless, after structural analysis, we conclude that in certain circumstances this possibility is worth considering.



Our calculations show a close relationship between g-shift and the local structure of the paramagnetic center with axial symmetry. Simple g-shift model, proposed by D J. Newman, can give important information about positions or displacements of paramagnetic ions in the case of paramagnetic centers with axial symmetry.

**Author Contributions:** Conceptualization, T.B. and S.M.K.; calculations, T.B.; EPR measurements and calculations, S.M.K.; visualization, T.B.; critical discussion, S.M.K.; literature, S.M.K.; writing—original draft preparation, T.B.; writing—review and editing, S.M.K. All authors have read and agreed to the published version of the manuscript.

**Conflicts of Interest:** The authors declare no conflict of interest.

## Appendix A

Coordination factors  $K_{\alpha\beta}$  are given by equations [20]:

$$\begin{aligned} K_{zz}[\theta] &= \sin^2\theta \\ K_{xx}[\theta, \Phi] &= 1 - \sin^2\theta\cos^2\Phi \\ K_{yy}[\theta, \Phi] &= 1 - \sin^2\theta\sin^2\Phi \end{aligned} \quad (\text{A1})$$

$$\begin{aligned} K_{xy}[\theta, \Phi] &= K_{yx}[\theta, \Phi] = -\sin^2\theta\sin\Phi\cos\Phi \\ K_{zx}[\theta, \Phi] &= K_{xz}[\theta, \Phi] = -\frac{1}{2}\sin 2\theta\cos\Phi \\ K_{zy}[\theta, \Phi] &= K_{yz}[\theta, \Phi] = -\frac{1}{2}\sin 2\theta\sin\Phi \end{aligned} \quad (\text{A2})$$

## References

- Sleight, A.W. Accurate Cell Dimensions for  $\text{ABO}_4$  Molybdates and Tungstates. *Acta Cryst.* **1972**, *B28*, 2899. [\[CrossRef\]](#)
- Cerný, P.; Jelínková, H.; Basiev, T.T.; Zverev, P.G. Highly efficient picosecond Raman generators based on the  $\text{BaWO}_4$  crystal in the near infrared, visible, and ultraviolet. *IEEE J. Quantum Electron.* **2002**, *38*, 1471–1478. [\[CrossRef\]](#)
- Mikhailik, V.B.; Kraus, H. Performance of scintillation materials at cryogenic materials. *Phys. Status Solidi B* **2010**, *247*, 1583–1599. [\[CrossRef\]](#)
- Voronina, I.S.; Ivleva, L.I.; Basiev, T.T.; Zverev, P.G.; Polozkov, N.M. Active Roman media:  $\text{SrWO}_4:\text{Nd}^{3+}$ ,  $\text{BaWO}_4:\text{Nd}^{3+}$ , growth and characterization. *J. Optoelectron. Adv. Mater.* **2003**, *5*, 887–892.
- Jinsheng, L.; Hangying, Y.; Shaoan, Y.; Jinlong, J.; Bao, Q.; Haiping, H.; Herui, W.J. Synthesis and luminescence properties of  $\text{BaWO}_4:\text{Pr}^{3+}$ . *Rare Earths* **2011**, *29*, 623–626.
- Su, Y.G.; Li, L.P.; Li, G.S. Synthesis and optimum luminescence of  $\text{CaWO}_4$ -based red phosphors with codoping of  $\text{Eu}^{3+}$  and  $\text{Na}^+$ . *Chem. Mater.* **2008**, *20*, 6060. [\[CrossRef\]](#)
- Kaczmarek, S.M.; Witkowski, M.E.; Głowacki, M.; Leniec, G.; Berkowski, M.; Kowalski, Z.W.; Makowski, M.; Drozdowski, W.  $\text{BaWO}_4:\text{Pr}$  single crystals co-doped with Na. *J. Cryst. Growth* **2019**, *528*, 125264. [\[CrossRef\]](#)
- Leniec, S.G.; Kaczmarek, T.; Bodziony, H.; Fuks, Z.; Kowalski, M.; Berkowski, M. Site symmetries of cerium ions in  $\text{BaWO}_4$  single crystals codoped with sodium ions. *Appl. Magn. Reason.* **2019**, *50*, 819–833. [\[CrossRef\]](#)
- Kaczmarek, S.M.; Leniec, G.; Bodziony, T.; Fuks, H.; Kowalski, Z.; Drozdowski, W.; Berkowski, M.; Głowacki, M.; Witkowski, M.E.; Makowski, M.  $\text{BaWO}_4:\text{Ce}$  Single Crystals Codoped with Na ions. *Crystals* **2019**, *9*, 28. [\[CrossRef\]](#)
- Cavalcante, L.S.; Sczancoski, J.C.; Lima, L.F., Jr.; Espinosa, J.W.M.; Pizani, P.S.; Varela, J.A.; Longo, E. Synthesis, characterization, anisotropic growth and photoluminescence of  $\text{BaWO}_4$ . *Cryst. Growth Des.* **2009**, *2*, 1002–1012. [\[CrossRef\]](#)
- Liu, L.; Zhang, S.; Mark, E.; Bowden, J.C.; de Yoreo, J.J. In Situ TEM and AFM Investigation of Morphological Controls during the Growth of Single Crystal  $\text{BaWO}_4$ . *Cryst. Growth Des.* **2018**, *18*, 1367–1375. [\[CrossRef\]](#)
- Rangappa, D.; Fujiwara, T.; Yoshimura, M. Synthesis of highly crystallized  $\text{BaWO}_4$  films by chemical reaction method at room temperature. *Solid State Sci.* **2006**, *8*, 1074–10178. [\[CrossRef\]](#)

13. Yu, H.; Hu, D.; Zhang, H.; Wang, Z.; Ge, W.; Xu, X.; Wang, J.; Shao, Z.; Jiang, M. Picosecond stimulated Raman scattering of BaWO<sub>4</sub> crystal. *Opt. & Laser Technol.* **2007**, *39*, 1239–1242.
14. Kunti, A.K.; Patra, N.; Sharma, S.K.; Swart, H.C. Radiative transitions probability of white light emitting Dy<sup>3+</sup> and K<sup>+</sup> codoped BaWO<sub>4</sub> phosphors via charge compensation. *J. Alloys Compd.* **2018**, *735*, 2410–2422. [[CrossRef](#)]
15. Zhang, T.H.; Liu, Q.; Zhang, X.; Wang, X.; Guo, M.; Song, J. First-principles study on electronic structures and color centers in BaWO<sub>4</sub> crystal with barium vacancy. *Phys. B* **2009**, *404*, 1538–1543. [[CrossRef](#)]
16. Zhang, H.; Liu, T.; Zhang, Q.; Wang, X.; Yin, J.; Song, M.; Guo, X. First-principle study on electronic structures of BaWO<sub>4</sub> crystals containing F-type color centers. *J. Phys. Chem. Solids* **2008**, *69*, 1815–1819. [[CrossRef](#)]
17. Chauhan, A.K. Czochralski growth and radiation hardness of BaWO<sub>4</sub> crystals. *J. Cryst. Growth* **2003**, *254*, 418. [[CrossRef](#)]
18. Newman, D.J.; Urban, W. Interpretation of S-state ion in EPR spectra. *Adv. Phys.* **1975**, *24*, 793. [[CrossRef](#)]
19. Wu, S.-Y.; Zheng, W.-C. EPR parameters and defect structures for two trigonal Er<sup>3+</sup> centers in LiNbO<sub>3</sub> and MgO or ZnO codoped LiNbO<sub>3</sub> crystals. *Z. Phys. Rev. B* **2002**, *65*, 224107.
20. Newman, D.J. On the g-shift of the S-state ions. *Phys. C Solid State Phys.* **1977**, *10*, L315. [[CrossRef](#)]
21. Bodziony, T. The relationship between the g-shift and the local structure for the axial impurity centers in the doped LiNbO<sub>3</sub> crystals. *J. Alloys Compd.* **2010**, *489*, 304–309. [[CrossRef](#)]
22. Abragam, A.; Bleaney, B. *Electron Paramagnetic Resonance of Transition Ions*; Clarendon Press: Oxford, UK, 1970.
23. Rudowicz, C. On the derivation of the superposition model formulae using the transformation relation for the Stevens operators. *Magn. Reson. Rev.* **1987**, *13*, 1.
24. Shao-Yi, W.; Hui-Ning, D. Theoretical investigations of the EPR g factors and the local structure for Er<sup>3+</sup> in BaWO<sub>4</sub>. *Spectrochim. Acta Part A* **2004**, *60*, 1991–1994. [[CrossRef](#)] [[PubMed](#)]
25. Shannon, R.D. Revised Effective Ionic Radii and Systematic Studies of Interatomic Distances in Halides and Chalcogenides. *Acta Cryst.* **1976**, *A32*, 751. [[CrossRef](#)]



© 2020 by the authors. Licensee MDPI, Basel, Switzerland. This article is an open access article distributed under the terms and conditions of the Creative Commons Attribution (CC BY) license (<http://creativecommons.org/licenses/by/4.0/>).